



## Vision Based Runway Detection and Alignment for UAV

Ravichandraprasad HG  
M-Tech (E&C), KIT, VTU,  
Karnataka, India

---

**Abstract**— *This paper presents the design and implementation of a synthetic vision overlay for UAV auto land procedures that is intended for conformance and integrity monitoring during final approach. In this Synthetic Vision (SV) technology provides the opportunity to use conformally integrated guidance reference image data to aligning of the UAV for proper alignment to the runway to auto land an aircraft system using the imagery of the nose-mounted camera. A potential use of this is to support the operator in determining whether the vehicle is flying towards the correct location in the real world, for example the desired touchdown position on the runway.*

**Keywords**— *Unmanned Aerial Vehicle (UAV), Synthetic Vision (SV), Auto land, Alignment, Camera*

---

### I. INTRODUCTION

An Unmanned Aerial Vehicle (UAV) is defined as a drone that is flying without a pilot in command board and well and fully remotely controlled from another location (floor, another aircraft, space) or programmed and fully autonomous. These include sensors and payloads, order and control information connects the operator station, the ground support equipment and equipment needed to launch and recover operations and maintenance, among others. UAVs are active area of research for many years and become attractive for civil applications. It is because of their ability to carry out what is known as tasks D3 (dull, dangerous and dirty).

In manned aviation, a reason for the development of an auto land capability is to be able to land in reduced visibility. This capability, over the years has been provided by the Instrument Landing System (ILS) Cat III under zero visibility conditions. The instrument landing system (ILS) however is very expensive and economically it is not feasible to provide ILS at all airports. To minimize the cost, aircraft-based technologies are being envisaged to provide equivalent visual operations (EVO) as the concept for the next generation air transportation system. For Unmanned Aerial Vehicles (UAVs), autonomous forms of auto land are being pursued to alleviate the need of special ground-based equipment for the generation of the reference path to a runway. Typically, this is done by using runway location data from an onboard database to generate the reference path to the desired location.

The much research can be done by Maximiliano Laiacker [1] presents an automatic landing system of multiple sensors combining visual detection on the track and the GPS guided approach is presented. The two main parts of the aircraft controller system are high precision and vision based detection algorithm track. Paul Williams, Michael Crump [2] Intelligent landing system is a vital to be fused into unmanned aeronautical vehicles later on component. It permits the UAV to recover beforehand obscure runways and execute exact independent arrivals.

Jiajia Shang, Zhongke Shi [3] is to solve the problems of recognition runway when landing UAV is this work a method of self-discovery based on land area and presents characteristic points, making full use of the track information and reduce time Hough transform. The combination of the Hough transform and least square fitting is applied to ensure the accuracy of extracting the boundaries of the court. Mr. Harper [4] is to produce a framework for finding a UAV on a runway using only one sensor of the camera. Our strategy is one fait projective geometry that uses a camera view to improve the estimation result of the position in this circumstance.

Jeremy Vezinet [5] presents a method based on video navigation, taking into account the properties and characteristics of a navigation system based on video is proposed. This part aims to provide a first stage of the feasibility study of a landing system based on video planes. Yunji Zhao Hailong Pei Zhou Hong [6] is work on Cam shift and SURF calculation diminishes the computational prerequisites. This calculation is exceptionally helpful for UAV independent landing framework. Bourquardez Odile and François Chaumette [7] proposed a scheme to align visual control of an aircraft relative to a runway. Uses linearized model of the aircraft and dissociated visual characteristics.

Patrick Rives [8] is taking into account homography for self-adjust and arriving of a flying machine was proposed. Likui Zhuang, Han Yadong, Fan Yanming [9] Keeping in mind the end goal to accomplish the target of the self-governing landing settled wing unmanned airborne vehicles (UAV), another strategy is proposed to utilize the monocular camera on board to give the data expected to landing. Courtney, Sharp, Omid Shakernia, and Shankar Sastry [10] have introduced a configuration usage of a real vision framework to land UAV in white arrival time. A few parts of our framework work particularly well.

### II. IMAGE PROCESSING FOR UAV APPLICATION

Here shows the how information can be extracted from a captured image frame. Image processing is an active area of research in its own right as it can be challenging to reliably extract large amounts of data efficiently and computationally.

### A. Runway Detection

Before identifying the track, it is important to analyze the characteristics of the track. When the UAV's landing, the camera is set in the nose and parallels shaft of light in the body axis.

### B. Pre-Processing

Image processing is applied to images based on the requirement of the algorithm. The image obtained from the camera is loud and image capture is poor. Therefore work with binary images for reducing processing costs and improve efficiency of algorithm. Images are initially changed over to gray scale by dispensing with hue and saturation data.

This is achieved by Equation

$$Y = 0.299 * R + 0.587 * G + 0.114 * B$$

Where Y is luminance and R, G, B speak to an estimation of red, green and blue picture individually.

### C. Median Filter

The median filter regards every pixel in an image on the back and looks at its close neighbours to decide whether or not representative of it in their environment. Instead of simply replacing a pixel value with an average of the values of neighbouring pixels, it is replaced with the median values.

### D. Detection of Edges

Edges describe limits are hence a matter of urgent significance in picture arrangement. The edges in the picture are territories with solid force differentiation hop in the power of a pixel to next pixel. In essential terms the slope of the picture power at every point is ascertained, so that the course of the biggest conceivable increment from light to dim and the rate of rotation in that heading.

Canny Edge Detector: With a perspective to the usage of the Canny edge identifier calculation, the need to take after various steps. The most vital step is to sift through all the commotion in unique picture before attempting to find and distinguish all sides.



Figure 1: Different edge operator original grayscale Image of the runway and detection by canny edge operator

## III. ALIGNMENT OF IMAGES

We will require connection of two or more images to extract information from them. For example if two consecutive frames in a video sequence taken from a moving camera can be connected, it is possible to obtain information about the depth of objects in environment and speed camera. These points are called points of interest and with a detector landmark. Find the relationship between images below using only these points.

### A. Harris Corner Detection

Harris angle indicator is a point identifier mainstream interest because of the strong immutability of rotation, scale, changes in lighting and noise. Harris corner detection is based on autocorrelation function of a signal on the spot, if the auto-correlation function of local measures local signal changes patches displaced by small amount in different directions. Given an image  $I(X) = I(x, y)$  where I indicates the intensity and  $X = (x, y)$  is the pixel horizontal and vertical position.

- Choose a window W with fixed size, e.g.,  $5 \times 5$ , and a threshold  $T \in \mathbb{R}$ .
- Compute the image gradient  $\nabla I = (I_x, I_y) = (g_x * I, g_y * I)$ , for example, using the Sobel operator.
- At all pixels within the window of W centered a  $(x, y)$ , compute a  $2 \times 2$  matrix.

$$G = \begin{pmatrix} \sum I_x^2 & \sum I_x I_y \\ \sum I_x I_y & \sum I_y^2 \end{pmatrix}$$

- Smallest eigen value method: if the smallest singular value  $\min \min(\sigma_i(G)), i=(1 \ 2)$  is greater than T, the pixel  $(x, y)$  is regarded as a corner point candidate.
- Check uniqueness condition: if the pixel  $(x, y)$  has greatest  $\min(\sigma_i(G))$  in a neighborhood, mark  $(x, y)$  as a corner point and eliminate the other false alarmed candidate in the neighborhood.

### B. Normalized Cross-Correlation (NCC)

Normalized cross correlation is discovered application an extensive variety in PC vision assignments, for example, stereo vision, movement following, and so on. Normalized cross-correlation is the easiest yet successful strategy as likeness measure that is invariant to linear brightness variations and contrast. It is simple equipment execution makes it helpful for applications in real time.

The normalized cross-correlation can be more efficiently processed images even when the rotational and a large scale. First points of interest can be found in the two pictures independently. Every purpose of hobby is appointed to the trademark size and the predominant bearing.

NCC matching: for each corner point  $X_i$ , ( $i = 1, 2, \dots, N1$ ),

(a) Compute the NCC value with all the feature point  $X' j$  ( $j = 1, 2, \dots, N2$ ) in the camera picture by

$$NCC(i, j) = \frac{\sum_w (I_1(\tilde{X}) - \bar{I}_1)(I_2(\tilde{X}') - \bar{I}_2)}{\sqrt{\sum_{w(x_i)} (I_1(\tilde{X}) - \bar{I}_1)^2 \sum_{w(x'_j)} (I_2(\tilde{X}') - \bar{I}_2)^2}}$$

Where  $\tilde{X} \in W(X_i), \tilde{X}' \in W(X'_j)$

$\bar{I}_1$  And  $\bar{I}_2$  are the mean intensities of the considerable number of pixels inside of the window and N total number of pixels.

(b) Determine the matched pointed  $X'_{j^*}$  by,

$$j^* = \arg \max(NCC(i, j))$$

$$j = (1, 2, \dots, N_2)$$

(c) If another correspondence  $(i', j^*)$  determined before, choose  $i_*$  is the matched point of  $j^*$  by

$$i_* = \arg \max(NCC(\hat{i}, j^*)),$$

$$\hat{i} = (i, i')$$

i.e., create one-to-one correspondence.

### C. Epipolar Geometry

The classical way to explain the concept of epipolar geometry is to consider the geometry in figure 2. Two pinhole cameras, located at positions  $O_1$  and  $O_2$ , are imaging the same world point X. The two cameras may be the same physical camera that has been moved or two different cameras, but the camera centre locations need to be distinct. The projection of the world point X on the two image planes will be at  $u_1$  and  $u_2$  respectively. But  $u_1$  will also be the image point for all points on the 3D line passing through  $O_1$  and X, e.g. the world points  $X'$  and  $X''$ . In the second camera, this 3D line will be imaged as the line  $l_2$  called an *epipolar line*. Repeating this process for other world points, it can be shown that all epipolar lines in the second image will intersect at a point  $e_2$  is the epipole. The epipole  $e_2$  also the image point in a second image of the camera center  $O_1$ .

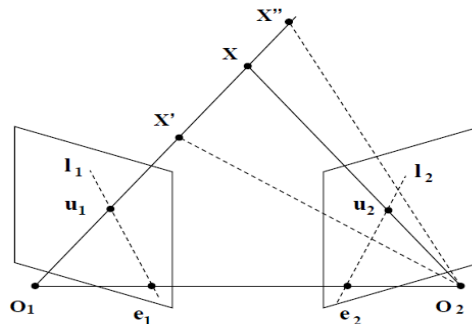


Figure 2: Epipolar geometry.

Confinement point in the first picture, the picture must lie in the epipolar line in the second picture, is called epipolar limitations, and can be scientifically communicated in

$$u_1^T l_2 = u_1^T F u_2 = 0.$$

F is fundamental matrix and 3x4 matrixes with seven degrees of freedom. A thorough mathematical derivation of the epipolar constraint and how the matrix F is related to the camera matrices  $C_1$  and  $C_2$ .

### D. RANSAC

The main idea behind RANSAC is easily explained estimating a best linear fit to a cloud of almost linear 2D points. Consider a set of points from a physical experiment where the expected relationship between two parameters is linear. Because of measurement errors is a spread around the waiting line and also there are some truly bad measurements, so called outliers. Using RANSAC to obtain a robust estimate of the line, two random points are chosen in the point cloud. A line between these two points is drawn. Accepted error distance of this line is defined and all points within the margin of error, the inliers constitute the consensus set. This process randomly picking two new points every time is repeated for a certain number of times, and the hypothesis of the line with the largest set of consensus is a robust estimate of the line. A baseline estimate at all points of the consensus set greater can be used to refine the estimate of the line.

**E. Direct Linear Transformation (DLT)**

The DLT algorithm for camera calibration is also a suitable technique for finding linear transformations between any two data sets given a certain number of points corresponding data between sets.

Normalized DLT: For the numerical calculation issues in the DLT algorithm, a normalization process should be applied.

This step is very important for less well conditioned problems such as DLT. Given  $n \geq 4$  point correspondences  $\vec{X}_i$  and  $\vec{X}'_i$ , a similarity transformation T1

$$T_1 = \begin{pmatrix} s & 0 & t_x \\ 0 & s & t_y \\ 0 & 0 & 1 \end{pmatrix}$$

Which consists of a translation and scaling will take points  $\vec{X}_i$  is a new set of points  $\vec{\tilde{X}}_i = T_1 \vec{X}_i$  such that centroid of new points is the coordinate  $(0,0)^T$  and their average distance from origin is  $\sqrt{2}$ .

Suppose  $\vec{X}_i = (x_i, y_i, 1)^T$ , we have

$$\vec{\tilde{X}}_i = T_1 \vec{X}_i = \begin{pmatrix} sx_i + t_x \\ sy_i + t_y \\ 1 \end{pmatrix} = \begin{pmatrix} \hat{x}_i \\ \hat{y}_i \\ 1 \end{pmatrix}$$

The centroid of  $\vec{\tilde{X}}_i$  is

$$\begin{pmatrix} \bar{\hat{x}}_i \\ \bar{\hat{y}}_i \\ 1 \end{pmatrix} = \begin{pmatrix} s\bar{x} + t_x \\ s\bar{y} + t_y \\ 1 \end{pmatrix} = (0, 0, 1)^T$$

Therefore,  $t_x = -s\bar{x}$  and  $t_y = -s\bar{y}$ .

The average distance between  $\vec{\tilde{X}}_i$  and origin is

$$\begin{aligned} & \frac{1}{n} \sum_i \sqrt{\hat{x}_i^2 + \hat{y}_i^2} \\ &= \frac{1}{n} \sum_i \sqrt{(sx_i - s\bar{x})^2 + (sy_i - s\bar{y})^2} \\ &= \frac{s}{n} \sum_i \sqrt{(x_i - \bar{x})^2 + (y_i - \bar{y})^2} \\ &= \sqrt{2}. \end{aligned}$$

Therefore, s can be computed as

$$s = \frac{\sqrt{2}}{\frac{1}{n} \sum_i \sqrt{(x_i - \bar{x})^2 + (y_i - \bar{y})^2}}$$

Similarly, a similarity transformation  $T_2$  will take points  $\vec{X}'_i$  is new set of points  $\vec{\tilde{X}}'_i = T_2 \vec{X}'_i$ . Apply DLT to correspondences of  $\vec{\tilde{X}}_i$  and  $\vec{\tilde{X}}'_i$  we obtain a homography  $\hat{H}$ . Since

$$\vec{\tilde{X}}'_i = H \vec{\tilde{X}}_i = T_2^{-1} \vec{\tilde{X}}'_i = T_2^{-1} \hat{H} \vec{\tilde{X}}_i = T_2^{-1} \hat{H} T_1 \vec{X}_i$$

This have the desired homography  $H = T_2^{-1} \hat{H} T_1$

**IV. RESULT**

The results were shown in this section. Original images show first, followed by the points of the detected corners (number of function points are indicated in the figure legends). In Figure NCC result, lines with different colors showing the correlation of pairs of points matched difference. The number of putative correspondences is indicated in Fig. In Fig result RANSAC, green dots and green lines show the inliers and red are the outliers. We can see from the figures that the RANSAC algorithm effectively remove these inaccurate matches. The latest figures are the image of the original scene and camera images processed using H obtained from four matches and all inliers. The reconstructed image of the scene using H obtained from all inliers is slightly closer to the image of the original scene. The root mean square error (MSE) between the original scene images transformed image and are listed in the figures. We can see that the transformed image obtained in H all inliers MSE has a lower value than that obtained from the 4 pairs.

**C. Input:**

Input is two images of the same scene with slight differences in rotation and translation between them. See Figure 3 below.

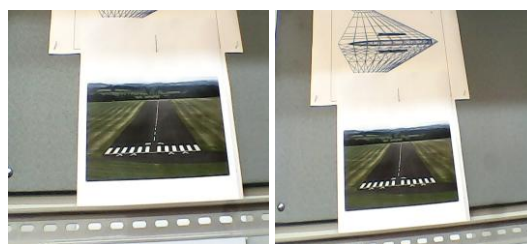


Figure 3: Two images of the same scene with small rotational angle

#### D. Harris Corner Detection

Corner points are extracted using Harris corner detector applied to both images see Figure 4 below.

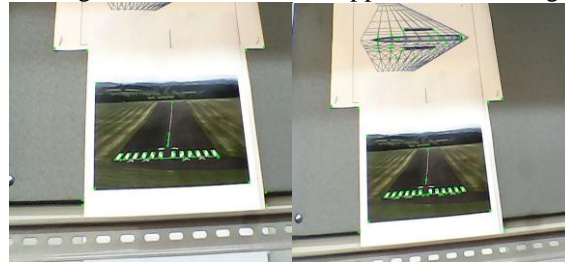


Figure 4: Detected Harris corners images

#### E. NCC and SSD Similarity Matching

Putative correlation between the set of corners taken in the first image and the second image are calculated and highlighted by comparing image neighbourhoods around the corner points using both NCC and SSD. See Figure 5 for the output results of NCC.

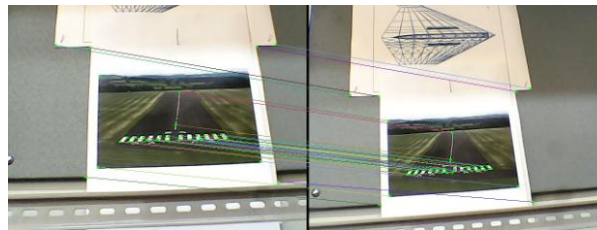


Figure 5: The result of correspondence matching using NCC. With tight threshold

#### F. RANSAC

RANSAC algorithm is used to estimate the homography between two images automatically selecting the correspondences (inliers) through an iterative procedure. Algorithm runs actually showing RANCSAC steps.

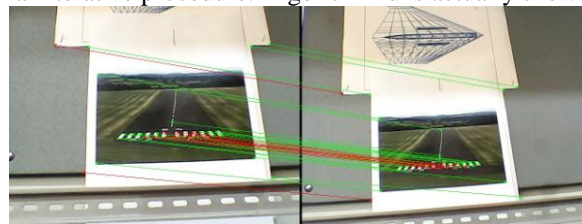


Figure 6: RANSAC matching inliers images

#### G. Output

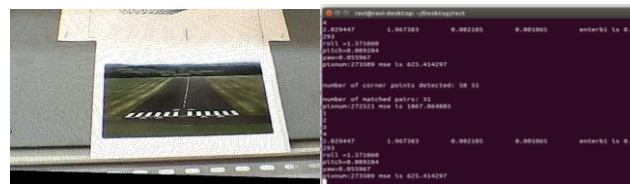


Figure 7: Final Results without Homography Refinement

### V. CONCLUSION

We have exhibited the configuration and execution of a constant vision-based framework for recognizing an arrival on runway and a controller to self-sufficiently arrive a UAV on the runway. The vision calculation is quick, strong and computationally economical. The arrival target has an all around characterized geometric shape and all the element purposes of the arrival target are coplanar.

#### REFERENCES

- [1] Maximilian Laiacker, Konstantin Kondak and Marc Schwarzbach, "Vision Aided Automatic Landing System for Fixed Wing UAV", *IEEE/RSJ International Conference on Intelligent Robots and Systems (IROS)*, ISSN: 2153-0858, pp.2971-2976, 2013.
- [2] Paul Williams, Michael, "Intelligent Landing System for Landing UAVS at Unsurveyed Airfields", *28TH International Congress of the Aeronautical Sciences ICAS*, 2012.
- [3] Jiajia Shang, Zhongke Shi, "Vision-based Runway Recognition for UAV Autonomous Landing", *IJCSNS International Journal of Computer Science and Network Security*, VOL.7, No.3, March 2007.
- [4] Andrew Miller, Mubarak Shah and Don Harper, "Landing a UAV on a Runway Using Image Registration", *IEEE International Conference on Robotics and Automation (ICRA)*, pp.182-187, May 2008.

- [5] Jeremy Vezinet, Anne-Christine Escher and Alain Guillet, “State of the art of image-aided navigation techniques for aircraft approach and landing”, *International Technical Meeting of The Institute of Navigation*, pp.473-607, Jan 2013.
- [6] Yunji Zhao, Hailong Pei and Hongbo Zhou, “Improved Vision-Based Algorithm for Unmanned Aerial Vehicles Autonomous Landing”, *International Conference on Medical Physics and Biomedical Engineering (ICMPBE2012)*, vol. 8, no. 2, pp.935-941, June 2012.
- [7] Odile Bourquardez and Francois Chaumette, “Visual Servoing of an Airplane for Alignment with respect to a Runway”, *IEEE International Conference on Robotics and Automation*, pp.1330-1335, 2006.
- [8] Tiago, Jos´e Azinheira and Patrick Rives, “Homography-based Visual Servoing of an Aircraft for Automatic Approach and Landing”, [\*IEEE International Conference on Robotics and Automation \(ICRA\)\*](#), pp.9-14, May 2010.
- [9] Likui Zhuang, Yadong Han and Yanming Fan, “Method of pose estimation for UAV is landing”, *Academy of Frontier Science Nanjing University of Aeronautics and Astronautics*, vol. 10, pp.S20401, 2012.
- [10] Courtney S, Sharp, Omid Shakernia S and Shankar Sastry, “A Vision System for Landing an Unmanned Aerial Vehicle”, *IEEE International Conference on Robotics and Automation*, vol. 2, pp.1720-1727, 2001.
- [11] [Daquan Tang](#), Naval Aeronaut and [Fei Li](#), “UAV attitude and position estimation for vision-based landing”, *Proceedings of the International Conference on Electronic and Mechanical Engineering and Information Technology*, vol. 9, pp.4446- 4450, August 2011.
- [12] Fitzgerald, Walker and Campbell, “A vision based forced landing site selection system for an autonomous UAV”, *Proceedings of the International Conference on Intelligent Sensor Networks and Information Processing*, pp.397-402, December 2005.
- [13] S.Saripalli, Montgomery and G. S. Sukhatme, “Vision-based autonomous landing of an unmanned aerial vehicle”, *Proceedings of the International Conference on Robotics and automation*, vol. 3, pp. 2799–2804, 2002.